J. Fluid Mech. (1989), *vol.* 206, *pp.* 47–73
Printed in Great Britain

Rotating stratified flow past a steep-sided obstacle: incipient separation

By M. R. FOSTER

Department of Aeronautical and Astronautical Engineering, The Ohio State University, 2036 Neil Avenue Mall, Columbus, OH 43210-1276, USA

(Received 21 October 1986 and in revised form 23 February 1989)

Many of the most interesting phenomena observed to occur in the flow of rotating and stratified fluids past obstacles, for example eddy shedding and wake unsteadiness, are due to separation of the boundary layer on the obstacle or its Taylor column. If the Rossby number of the flow lies between $E^{\frac{1}{2}}$ and E (E is the Ekman number) and the Burger number is small, the structure of a viscous shear layer of width $E^{\frac{1}{3}}$ on the circumscribing cylinder of an axisymmetric obstacle controls the inviscid flow. The surface boundary layer is not an Ekman layer, but a Prandtl layer, even at small Rossby numbers. As the slope of the obstacle at its base increases, the nature of the inviscid motion is altered substantially, in the rotation-dominated regime. We show that, for sufficiently large slopes, the flow develops a small region of non-uniqueness external to the column, simultaneously with the separation of the narrow band of fluid flowing round the base of the object.

1. Introduction

Over the past three decades, much effort has been devoted to the understanding of rotating and stratified flows over obstacles, both as they occur in nature in the atmosphere and oceans, and also as they are observed in laboratory situations. Baines & Davies (1980) have reviewed much of the work related to laboratory flows. Experimental programs for such flows were long rare in the literature, with Davies' (1972) paper the most definitive for a long time. More recently, Boyer and coworkers in Wyoming have made a number of careful experiments, reported for example in Boyer & Biolley (1986) and Boyer *et al.* (1987). The combined effects of rotation and stratification in these papers lead to a variety of interesting phenomena like eddy-shedding, separation, flow unsteadiness, etc. Hogg (1973), McCartney (1975), and Huppert (1975) presented theoretical models of the effects of stratification on Taylor columns. In each of these treatments, the height of the obstacle is small, and of the order of the Rossby number. More recently, Cheng, Hefazi & Brown (1984) have studied the far-field disturbances that arise in an unbounded rotating, stratified flow in the inviscid limit. Foster (1979*a*, *b*, 1982) has given solutions for slow flow of vertically confined fluids past two-dimensional obstacles, relieving the assumption that the obstacle height is small. Merkine (1985) has recently studied the flow past a vertical cylinder in a confined rotating, stratified fluid. The differences between his analysis and the present paper are discussed in detail in §2.

This paper presents solutions for rotating and stratified flow past large obstacles, since Boyer & Chen (1987) quite properly point out that laboratory studies must be done with obstacles of large height, in order to simulate what happens in orographic flows in the atmosphere. Several parameters, the Rossby number, Ekman number,

Prandtl (or Schmidt) number, and Burger number, characterize the flow. We investigate the flow with a view toward the possible separation and the formation of eddies or unsteadiness. The case discussed herein is for small Burger numbers, that is, the flow is dominated by rotation effects, with the stratification effects relatively weaker. Let the fluid velocity past the object be U, and the fluid layer depth be h; ν is the kinematic viscosity, and $\Delta\rho^*/\rho_0^*$ is the dimensionless density difference across the layer. If the rotation rate is denoted by Ω, then the Burger number, $S = g\Delta\rho^*/(\Omega^2\rho_0^* h)$; the Rossby number, $Ro = U/\Omega h$; and the Ekman number, $E = \nu/\Omega h^2$. The restrictions on the following analysis are:

$$S = o(1), \quad Ro = O(SE^{\frac{1}{2}}), \quad \sigma S \gg E^{\frac{1}{2}},$$

where σ is the Schmidt number. It follows that the Rossby number is small compared with $E^{\frac{1}{2}}$. It is well known (Walker & Stewartson 1974) that for an homogeneous rotating flow, the flow is attached until Ro is a particular order-one multiple of $E^{\frac{1}{2}}$. What we discover here is that, in spite of the relatively small amount of stratification with S small, as the slope of the obstacle where it meets the lower wall increases, some difficulties arise in what was a well-behaved solution at moderate slopes.

In the parameter range under study here, the flow away from the obstacle is inviscid and obeys a coupled pair of nonlinear equations whose solution involves matching through a thin $E^{\frac{1}{6}}$ layer surrounding a 'Taylor column' to a flow over the top of the obstacle that is also nonlinear, owing to the large height of the object. If $\lambda \equiv E^{\frac{1}{2}}S/Ro$, then the problem is formulated for arbitrary values of λ. Relatively large values of λ correspond to larger stratification effects, and small values to larger rotation effects.

The physics of the flow in the parameter range under study here is relatively simple. In front of the obstacle, suppose the fluid moves laterally. The lateral motion causes fluid to be pumped out of the Ekman layers. That vertical interior motion lifts the isopycnics of the linear stratification, which, by the energy equation, is balanced by horizontal convection of a baroclinic density perturbation if $\lambda = O(1)$. That density perturbation, since it is baroclinic, produces additional vertical vorticity which increases the lateral motion (thermal wind!), and so on.

A crucial point of this paper is in §3, where we point out that the boundary layer on the surface of this large obstacle is *not* an Ekman layer (unless the slopes are very small), because the production of new vorticity out of the baroclinicity of the flow in the layer adjacent to the object dominates the diffusion of vorticity off the wall. In such a case, the boundary-layer equation is the Prandtl equation even at these small Rossby numbers, because of the inherent nonlinearity of the density equation. The linearization of this equation that leads to Ekman layer/density layer combinations always requires small slopes or fortuitous shapes for which the nonlinear terms vanish identically (see Merkine 1985, for example). In fact, for reasonable values of the Prandtl (Schmidt) number, the Ekman layer is recovered when the surface has slope $E^{\frac{1}{6}}$.

In §4, the resultant boundary-layer structure leads to the equations for the outer flow, in particular the vertical shear. Those solutions are joined across the circumscribing cylinder of the obstacle, $r = a$, by means of conditions deduced in §5 from the structure of the nonlinear $E^{\frac{1}{6}}$ layer mentioned above. It is then possible to consider solutions in particular cases.

The large-λ flow, discussed in detail in §6, can be found easily only for small obstacle slopes, owing to the role played by the surface boundary layer. It is Stokes-

like (though the Reynolds number $Ro/E = S/E^{\frac{1}{2}}$ may be large!), with a non-uniformity in the far-field resolved by an Oseen limit there. The Oseen solution shows a narrow wake far downstream, with width $(\lambda x)^{\frac{1}{2}}$ (small compared with x for $x \gg \lambda$); x is the streamwise coordinate.

For small values of λ, the flow is strongly reminiscent of homogeneous flow past an obstacle; the pressure, which is a stream function for the geostrophic flow, is an harmonic function away from the Taylor column wall. However, there are narrow, rotational shear layers (where surface friction, but not lateral friction, is important) that sandwich the $E^{\frac{1}{3}}$ layer, as shown in detail in §7. The layers have widths $\lambda^{\frac{1}{2}}$ and $\lambda^{\frac{1}{4}}$ on the outside and inside of the column wall, respectively. All of the vertical velocity shear is confined to these regions. The vertical structure is intimately tied to the stratification, but these layers are neither Stewartson layers nor buoyancy layers (Barcilon & Pedlosky 1967).

In §8, we explore the question of what happens to the flow examined in §7 for $\lambda \ll 1$, if the object in the flow has very steep sides at its lowest point. For a spherical cap, we show that the solution structure is self-consistent for slopes up to size $\lambda^{-\frac{2}{5}}$. For slopes larger than $\lambda^{-\frac{2}{5}}$, but smaller than $\lambda^{-\frac{1}{2}}$, a tiny region of non-uniqueness develops in the outer shear-layer solution near the obstacle shoulder (the locations on the object where the surface normal is perpendicular to the upstream flow direction). At the same time, the boundary layer on the sloping surface under the interior shear layer separates under a severe adverse pressure gradient.

It is interesting to compare the nature of separation as it occurs here with what happens in the non-stratified case. Walker & Stewartson (1974) note that, for values of $Ro/E^{\frac{1}{2}}$ beyond a particular value, the outer shear layer on the Taylor column develops a point of zero shear at the rear stagnation point – so presumably at larger Rossby numbers the flow round the column separates from the top to the bottom of the column. On the other hand, in the case investigated here, the only problem that arises external to the column is the non-uniqueness in the outer shear layer; the separation, *per se*, occurs over the bump itself, and then only in a narrow band round the obstacle at its base. Having said that, it should be noted that the problem that arises in the exterior shear layer that leads to the non-uniqueness is not unlike what occurs at a point of zero skin-friction in a boundary layer, viz. the downstream variable ceases to be time-like and the problem becomes ill-posed. Clearly, proceeding to a proper solution in this case, and also for objects with still larger slopes, requires solving for the external flow together with the boundary layer, simultaneously, in ways that are now beginning to be understood (Smith 1985).

So, in summary, for strongly stratified flows ($\lambda \gg 1$), the nonlinear surface layer makes the entire $Ro \ll 1$ problem nonlinear for any objects but those with very small slopes; rotation-dominated flows ($\lambda \ll 1$) are fully attached, unless the obstacle slope at its base is larger than $\lambda^{-\frac{2}{5}}$.

So the requirements for non-separated flow, in terms of the object slope $f'(a)$, are

$$|f'(a)| \ll \frac{1}{\lambda}, \quad \lambda \gg 1$$

and

$$|f'(a)| \ll \frac{1}{\lambda^{\frac{2}{5}}}, \quad \lambda \ll 1.$$

Finally, it seems that most workers in this field have regarded the Burger number,

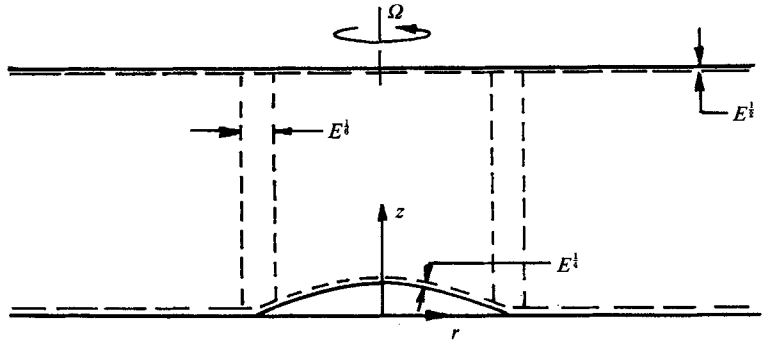

FIGURE 1. Geometrical configuration for the flow, showing the boundary layers and free-shear layer.

S, as the primary determiner of the relative importance of rotation and stratification. The work presented here suggests rather that the parameter

$$S\frac{E^{\frac{1}{2}}}{Ro}$$

is the important one for low-Ro flows.

2. Formulation and outer expansion

Consider a stratified fluid confined between horizontal, parallel planes, rotating about their common normal at angular velocity Ω, and flowing at speed U past an obstacle located on the lower plane (cf. figure 1). The planes are separated by a distance h. The non-dimensional Boussinesq equations are

$$\nabla\cdot\boldsymbol{u} = 0, \tag{2.1}$$

$$\epsilon Ro(\boldsymbol{u}\cdot\nabla)\boldsymbol{u} + 2\epsilon\boldsymbol{k}\times\boldsymbol{u} + \nabla p = \epsilon E\nabla^2\boldsymbol{u} - \rho\boldsymbol{k}, \tag{2.2}$$

$$\frac{Ro\sigma}{E}\boldsymbol{u}\cdot\nabla\rho = \nabla^2\rho, \tag{2.3}$$

where the velocity has been made non-dimensional with U, lengths with h, and the dimensional density ρ^* has been written as

$$\rho^* = \rho_0^* + \Delta\rho^*\rho,$$

where $\Delta\rho^*$ is the density difference across the planes. Ro is the Rossby number, $U/\Omega h$, and E, the Ekman number, $\nu/\Omega h^2$. The measure of the relative importance of the stratification and rotation is $S \equiv g\Delta\rho^*/\Omega^2\rho_0^* h$, and for convenience, the ϵ parameter in the equations is Ro/S. (This parameter S differs from that of Davies' 1972 by a factor of four.) σ is the Prandtl or Schmidt number, depending upon whether the density differences are due to thermal or salinity variations. It is convenient to use components for $\boldsymbol{u}$ in a cylindrical polar system; u in the radial (r) direction, v in the azimuthal direction (θ), and w vertical (z). Hence the z-direction is parallel to $\boldsymbol{\Omega}$, and $\boldsymbol{k}$ in (2.2) is $\boldsymbol{\Omega}/|\boldsymbol{\Omega}|$.

We suppose that the obstacle has shape given by

$$z = f(r) \quad \text{for } r < a, \quad f(a) = 0 \tag{2.4}$$

and has finite slope everywhere; in particular, $|f'(a)|$ is finite.

Far from the obstacle, we take the flow to be uniform and the density to be linearly stratified. Thus

$$\left.\begin{aligned} \boldsymbol{u} &\to \nabla x \\ \rho &\to -z \end{aligned}\right\} \quad \text{for } r \to \infty. \tag{2.5}$$

Other boundary conditions are imposed at the solid surfaces,

$$\boldsymbol{u} = \mathbf{0} \quad \text{on} \quad \begin{cases} z = 1, \\ z = 0,\ r > a, \\ z = f,\ r < a, \end{cases} \tag{2.6}$$

$$\rho = -1 \quad \text{on} \quad z = 1, \tag{2.7a}$$

$$\rho = 0 \quad \text{on} \quad z = 0,\ r > a, \tag{2.7b}$$

$$\rho = g(r) \quad \text{on} \quad z = f,\ r < a, \tag{2.7c}$$

or

$$\partial\rho/\partial n = 0 \quad \text{on} \quad z = f,\ r < a. \tag{2.7d}$$

$g(r)$ is the density distribution on the obstacle, and n is a normal to the obstacle surface. Where (2.7*c*) is concerned, arbitrary $g(r)$ causes convection near the obstacle so that the flow is a combination of that due to the uniform flow past the obstacle and that due to thermal or haline effects at the surface. Since the purpose of this paper is to study the nature of the forced flow, and not that due to obstacle heating, say, we make a special choice for $g(r)$, so that the boundary condition is

$$\rho = g(r) = -f(r) \quad \text{on} \quad z = f,\ r < a. \tag{2.8}$$

It is also true, of course, that for fluids stratified by salt in water, for example, the appropriate boundary condition is (2.7*d*); however, because such a no-flux condition alters substantially the nature of the boundary layers, no further consideration will be given in *this* paper to solutions under (2.7*d*). Hence, under (2.8), the exact solution $\boldsymbol{u} \equiv \mathbf{0}$, $\rho = -z$ of (2.1)–(2.3) satisfies all of the density boundary conditions (2.5*b*), (2.7), and (2.8). The implications of this assumption for the boundary-layer structure near $z = f$ will be dealt with in §3.

In proceeding to a solution of (2.1)–(2.3), (2.5)–(2.8), we suppose ϵ, Ro, and E are all small, so that the expansion proceeds as

$$\left.\begin{aligned} \boldsymbol{u} &= \boldsymbol{u}_1 + \epsilon\boldsymbol{u}_2 + \epsilon^2\boldsymbol{u}_3 + \ldots, \\ p &= p_0 + \epsilon p_1 + \epsilon^2 p_2 + \ldots, \\ \rho &= \rho_0 + \epsilon\rho_1 + \epsilon^2\rho_2 + \ldots. \end{aligned}\right\} \tag{2.9}$$

The first term in (2.2) introduces a term into the (2.9) series of $O(\epsilon Ro)$; if that term is to be small compared with the third term in (2.9), we require $Ro \ll \epsilon$, or $S \ll 1$. In addition, later in this section, we suppose that $\epsilon = O(E^{\frac{1}{2}})$, which means $Ro = O(SE^{\frac{1}{2}})$, and hence, $Ro \ll E^{\frac{1}{2}}$. The negligibility of the viscous term of (2.2) in the (2.9) solution requires $E \ll \epsilon$, so $Ro \gg SE$. Hence, the Rossby-number range for the validity of this analysis, and the S restrictions as well, are

$$SE \ll Ro \ll E^{\frac{1}{2}}, \quad S \ll 1. \tag{2.10}$$

The density transport equation imposes additional constraints on the flow, which are no more severe than that the Péclet number be large, which in the notation of this problem requires simply $\sigma Ro \gg E$, or in terms of the Burger number,

$$\sigma S \gg E^{\frac{1}{2}}, \tag{2.11}$$

so if σ is large, as for salt in water, this is easily satisfied; for $\sigma = O(1)$, there is a limit on the smallness of S.

Proceeding with the substitution of (2.9) into (2.1)–(2.3) leads to the first-order equations

$$\nabla p_0 + \rho_0 \boldsymbol{k} = 0, \quad \boldsymbol{u}_1 \cdot \nabla \rho_0 = 0 \tag{2.12}$$

whose solution, subject to (2.7), is

$$\rho_0 = -z, \quad w_1 = 0. \tag{2.13}$$

To next order, we have

$$\nabla \cdot \boldsymbol{u}_1 = 0 \tag{2.14a}$$

$$2\boldsymbol{k} \times \boldsymbol{u}_1 + \nabla p_1 + \rho_1 \boldsymbol{k} = 0, \tag{2.14b}$$

$$(\boldsymbol{u}_1 \cdot \nabla)\rho_1 - w_2 = 0, \tag{2.14c}$$

from which it is clear that p_1 is a stream function for (u_1, v_1). Finally, the $(\,)_2$ momentum equation is

$$2\boldsymbol{k} \times \boldsymbol{u}_2 + \nabla p_2 + \rho_2 \boldsymbol{k} = 0; \tag{2.15}$$

the z-component of the curl of this equation is

$$\frac{\partial w_2}{\partial z} = 0. \tag{2.16}$$

Using (2.14c), (2.16) leads to

$$(\boldsymbol{u}_1 \cdot \nabla)\frac{\partial^2 p_1}{\partial z^2} = 0,$$

whose general solution is

$$\frac{\partial^2 p_1}{\partial z^2} = F(p_1, z),$$

since p_1 is a stream function for $\boldsymbol{u}_1$. Comparing (2.9) with upstream conditions (2.5) shows $\rho_1 \to 0$ for $r \to \infty$, but $p_1 \to -2r\sin\theta$. Therefore, $F \equiv 0$ and the equation for p_1 becomes

$$\frac{\partial^2 p_1}{\partial z^2} = 0.$$

This work differs from Merkine's (1985) at just this point. He obtains, for the p_1 equation, a Laplace equation for $\partial^2 p_1/\partial z^2$. Thus, his analysis reflects a diffusion-dominated flow, and this work is convection-dominated. The difference appears in the appropriate parameter restriction here, (2.11), *vs.* Merkine's requirement that $\sigma S = O(E^{\frac{1}{2}})$. This analysis should be more appropriate to laboratory situations in which $\Delta\rho^*$ is due to salinity variations, because $\sigma \sim 1000$ in such a case. For Merkine's results, S would have to be $\sim 10^{-5}$ in any of Boyer's experiments, for example. Here, S-values of 0.1 can fit into the parameter restrictions if Ro is small. The general solution of the p_1 equation is

$$p_1 = A(r, \theta)z + B(r, \theta). \tag{2.17}$$

Noting from (2.17) and (2.14b) that

$$\rho_1 = -A \tag{2.18}$$

we see that (2.14c) gives $w_2 = -\boldsymbol{u}_1 \cdot \nabla A$, or

$$w_2 = \frac{1}{2}\frac{1}{r}\frac{\partial(A, B)}{\partial(r, \theta)}. \tag{2.19}$$

The interior dynamics imposes a rather strong structure, (2.17)–(2.19), on the flow, but leaves the functions A and B arbitrary. That arbitrariness is removed by the boundary layers above and below the flow, which are analysed in the subsequent section.

The most interesting case occurs when the vertical velocity driven by the Ekman outflow is of the same order as the $(\,)_2$ perturbation in the (2.9) series. That requirement leads to

$$E^{\frac{1}{2}} = \lambda\epsilon, \tag{2.20}$$

where λ is now an $O(1)$ parameter. Foster (1979*b*) investigated such a flow over a two-dimensional ridge.

Such a balance, making $\lambda = O(1)$, has a simple physical interpretation. Suppose that the fluid flows laterally in advance of the obstacle (upstream). That lateral motion causes fluid to be pumped out of the Ekman layers, lifting the isopycnics of the linear stratification, which, to hold the density of each fluid particle fixed, causes a baroclinic density perturbation. This baroclinic perturbation creates new vorticity which turns the flow, giving rise to more Ekman pumping, and so on. The process feeds on itself, and would seem to imply upstream influence in such flows.

3. Surface boundary layers

There is no question that the Ekman layers exist on horizontal surfaces in this parameter range, and also on $z = f(r)$ for f' sufficiently small; however, if $f'(r)$ is $O(1)$, the boundary layer is substantially different, and *not* in general an Ekman layer. What happens here is the following: near the sloping surface of the object, the pressure gradient must be parallel to that surface. That portion of the gradient that is vertical is balanced by the buoyancy term; the radial portion of the gradient balances the Coriolis force due to azimuthal motion. Hence, there is a simple geometrical relationship between the azimuthal velocity and the baroclinic density perturbation. This relationship must exist unless the surface slope is so small that the vertical pressure gradient component is negligible by comparison with the radial viscous forces – in that case an Ekman layer arises. The derivation given below seems the simplest.

Now, the form of the bondary layer on the surface, since it turns out to be nonlinear, depends on the magnitude of the velocity vector in the inviscid flow above the surface. Here, we must anticipate the results found in §4, which show that

$$u_1 = -\tfrac{1}{2}(z-f)\frac{\partial A^-}{\partial\theta}, \quad v_1 = \frac{1}{2}\left[(z-f)\frac{\partial A^-}{\partial r} - f'(r)A^-\right]. \tag{3.1}$$

Thus, to match to a layer of width δ in $z-f$, we see that u is $O(\delta)$, but v has both $O(\delta)$- and $O(f')$-terms. This is important in what follows.

Note that the z-component of the curl of (2.2) is

$$-2\frac{\partial w}{\partial z} = E\nabla^2\omega, \tag{3.2}$$

where $\omega = \boldsymbol{k}\cdot(\boldsymbol{\nabla}\times\boldsymbol{u})$ and nonlinear terms are neglected for Ro sufficiently small. If we put $\rho = \rho_0 + \rho'$, where $\rho_0 = -z$, into the energy equation (2.3), then eliminate $\partial w/\partial z$ from this equation and (3.2), we obtain

$$\frac{\partial}{\partial z}[\boldsymbol{u}\cdot\boldsymbol{\nabla}\rho'] = \tfrac{1}{2}E\nabla^2\left[\frac{2}{\sigma Ro}\frac{\partial\rho'}{\partial z} - \omega\right]. \tag{3.3}$$

Apart from the neglect of the nonlinearity in (2.2), no other approximation has been made in (3.2). It is convenient for analysing the boundary layers to write (3.2) in an (r, θ, n) system, rather than (r, θ, z), where $n \equiv z - f(r)$; the new system is clearly non-orthogonal. Under such a transformation, (3.3) becomes

$$\frac{\partial}{\partial n}[\boldsymbol{u}\cdot\nabla\rho'] = \tfrac{1}{2}E\nabla^2\left[\frac{2}{\sigma Ro}\frac{\partial\rho'}{\partial n} + f'\frac{\partial v}{\partial n} - \omega'\right], \tag{3 4}$$

where $\omega' = (1/r)(rv)_r - (1/r)u_\theta$, where the r-derivative is now understood to be taken at fixed n and θ. If we now make a boundary-layer approximation in retaining only n-derivatives in ∇^2, (3.4) becomes

$$\frac{\partial}{\partial n}[\boldsymbol{u}\cdot\nabla\rho'] = \tfrac{1}{2}E(1+(f')^2)\frac{\partial^2}{\partial n^2}\left[\frac{2}{\epsilon\sigma S}\frac{\partial\rho'}{\partial n} + f'\frac{\partial v}{\partial n} - \omega'\right], \tag{3.5}$$

where Ro has been replaced by $S\epsilon$. In this coordinate system, note that the nonlinear term in (3.5) is

$$\boldsymbol{u}\cdot\nabla\rho' = u\frac{\partial\rho'}{\partial r} + \frac{v}{r}\frac{\partial\rho'}{\partial\theta} + [1+(f')^2]^{\frac{1}{2}}\bar{w}\frac{\partial\rho'}{\partial n}, \tag{3.6}$$

where $\bar{w} \equiv (w - f'u)/[1+(f')^2]^{\frac{1}{2}}$ is the velocity component normal to the surface. The continuity equation (2.1) is given by

$$\frac{1}{r}\frac{\partial(ru)}{\partial r} + \frac{1}{r}\frac{\partial v}{\partial\theta} + [1+(f')^2]^{\frac{1}{2}}\frac{\partial\bar{w}}{\partial n} = 0. \tag{3.7}$$

The momentum equations in that thin layer, on eliminating the pressure, take the following form:

$$\frac{\partial}{\partial n}(f'\rho' - 2\epsilon v) - \frac{\partial\rho'}{\partial r} = \lambda\epsilon^3 D\left(\frac{\partial u}{\partial n} + f'\frac{\partial w}{\partial n} - \frac{\partial w}{\partial r}\right), \tag{3.8a}$$

$$2\epsilon\frac{\partial u}{\partial n} - \frac{1}{r}\frac{\partial\rho'}{\partial\theta} = \lambda\epsilon^3 D\left(\frac{\partial v}{\partial n} - \frac{1}{r}\frac{\partial w}{\partial\theta}\right), \tag{3.8b}$$

where we have written, for shortness, D for $[1+(f')^2]^{\frac{1}{2}}\partial^2/\partial n^2$. From these equations, it is evident that so long as, for the moment, we take the layer width to be larger than the Ekman width, ϵ, the 'thermal wind' terms on the left dominate. In addition, notice that, provided the slope, f', is much larger than the layer thickness, δ, the first two terms in (3.8a) are dominant, and integrate to

$$\rho' = \frac{2\epsilon}{f'}v. \tag{3.9}$$

Also, then, (3.8b) becomes

$$\frac{\partial\hat{u}}{\partial y} + \frac{1}{r}\frac{\partial v}{\partial\theta} = 0, \tag{3.10}$$

where y is now a scaled boundary-layer coordinate, n/δ, with δ yet to be found, and

$$u = -\frac{\delta}{f'}\hat{u}. \tag{3.11}$$

Combining (3.9) and (3.10) with (3.11), we obtain the boundary-layer equation

$$\hat{u}\frac{\partial v}{\partial y} + \frac{v}{r}\frac{\partial v}{\partial\theta} - \left(\frac{v}{r}\frac{\partial v}{\partial\theta}\right)_{\mathrm{e}} = \frac{\lambda^2\epsilon}{\delta^2}(1+(f')^2)\left[\tfrac{1}{4}(f')^2 + \frac{1}{\sigma S}\right]\frac{\partial^2 v}{\partial y^2}. \tag{3.12}$$

The subscript e refers to conditions at the boundary-layer edge. Notice that, since the leading-order matching conditions and boundary conditions are satisfied for v and ρ, there is not need for any other boundary layer – this is a combined thermal/dynamical layer. The only restrictions, to be checked *a posteriori*, are that the thickness, δ, be small compared to the slope of the surface, f', but large compared to the Ekman thickness, ϵ.

Equation (3.12) is the familiar Prandtl boundary-layer equation. The thickness δ depends not only on λ and ϵ, but also on the local slope $f'(r)$ and the size of σS. It is also very important that (3.12), notwithstanding (3.9), does *indeed* include effects of viscosity on the fluid momentum; recall that we began with (3.2). In what follows, we explore the various forms of the volumetric flow rate, depending on the parameters of the problem, for sufficiently large f'. We shall have to reinvestigate this limit for small slopes.

$$f' = O(1)$$

If the surface slope, f', is $O(1)$, then so long as σS is $O(1)$ or smaller, depending on the size of σ, we may choose $\delta = \lambda(\epsilon/\sigma S)^{\frac{1}{2}}$ in (3.12). Equation (3.10) indicates that the volumetric flow rate in the radial direction is given by

$$\mathscr{f} \equiv \int_0^\infty (u-u_e)\,\mathrm{d}n = -\frac{\lambda^2\epsilon}{\sigma S}\frac{1}{r}\frac{\partial}{\partial\theta}\int_0^\infty y(v-v_e)\,\mathrm{d}y. \tag{3.13}$$

So the flow rate is $O(\epsilon)$, for $\sigma S = O(1)$, just as it would be for an Ekman layer, but of course the dynamics are radically different. If, on the other hand, σ is $O(1)$, then the flow rate is clearly somewhat larger.

$$|f'| \gg 1$$

Now the matching condition for v in (3.12) is $v \to v_e$ for $y \uparrow \infty$. Noting, from (3.1), that $v_e = O(|f'|)$, and using $|f'(a)|$ as characteristic of the scale of f' for all r, for $|f'| \to \infty$, $\delta = \lambda\epsilon^{\frac{1}{2}}|f'(a)|^{\frac{3}{2}}$, provided that S is not so small that the $1/\sigma S$-term dominates the $(f')^2$ term. Examination of the equivalent of (3.13) in this case shows that the flow rate scales like $\lambda^2\epsilon|f'(a)|^3$. These scales are crucial to the discussion in subsequent sections. Thus,

$$\mathscr{f} = \lambda^2\epsilon|f'(a)|^3 Q \tag{3.14}$$

in symbolic form, where Q is the $O(1)$ integral of (3.12), which is then valid for

$$\sigma S \gg 1/|f'(a)|^2.$$

$$f' = o(1)$$

As indicated above, the arguments leading to (3.12) fail unless f' is larger than the boundary-layer thickness, δ. The thickness of the small-f' layer is strongly dependent on the size of σ. If the fluid is essentially non-diffusive, then (3.12) shows that $\delta = \lambda(\epsilon|f'(a)|)^{\frac{1}{3}}$. In such a case, the flux is order $\epsilon f'$. The requirement that f' be much larger than the thickness, then, requires that $|f'(a)| \gg E^{\frac{1}{2}}$ – so the Ekman scales reappear when $f'(a) = O(E^{\frac{1}{3}})$. However, this case seems not very relevant to geophysical or laboratory situations, since it requires that $\sigma S \gg 1/|f'|^2$ – not very likely for small S!

On the other hand, if the σS-term is dominant on the right-hand side of (3.12), then the thickness, δ, turns out to be $\lambda\{\epsilon/(\sigma S|f'(a)|)\}^{\frac{1}{2}}$, and the flux law becomes

$$\mathscr{f} = \frac{\lambda^2\epsilon}{|f'|\sigma S}Q, \tag{3.15}$$

again written symbolically with all of the complication buried in Q, which is $O(1)$. However, the requirement that f' be large compared with δ is much more restrictive, hence the two constraints on this small-$|f'(a)|$ flux law, (3.15) are

$$|f'(a)| \leqslant (1/\sigma S)^{\frac{1}{2}}, \quad |f'(a)| \gg \lambda^{\frac{2}{3}}(\epsilon/\sigma S)^{\frac{1}{3}}. \tag{3.16}$$

So, the restrictions are severe, and (3.12) fails, for small slopes, at f' values of $E^{\frac{1}{6}}$, for σS of order one.

With the choices for δ as specified above, then, (3.9) and (3.11) become

$$\frac{\partial \hat{u}}{\partial y} + \frac{1}{r}\frac{\partial \hat{v}}{\partial \theta} = 0, \tag{3.17a}$$

$$\hat{u}\frac{\partial \hat{v}}{\partial y} + \frac{\hat{v}}{r}\frac{\partial \hat{v}}{\partial \theta} - \left(\frac{\hat{v}}{r}\frac{\partial \hat{v}}{\partial \theta}\right)_e = H(r)\frac{\partial^2 \hat{v}}{\partial y^2}, \tag{3.17b}$$

where $\hat{v} = -v/f'(a)$, and $H(r)$ depends upon the f' parameter range, *viz.*

$$H(r) = 1, \quad |f'(r)| \ll 1, \tag{3.18a}$$

$$H(r) = [1 + \{f'(r)\}^2][1 + \tfrac{1}{4}\sigma S\{f'(r)\}^2], \quad |f'(r)| = O(1), \tag{3.18b}$$

$$H(r) = [f'(r)/f'(a)]^4, \quad |f'| \gg 1. \tag{3.18c}$$

Actually, of course, the quantity H may be absorbed into the definition of the y-coordinate, and clearly has the effect of providing some radial variation to the boundary-layer thickness. The obvious thing suggested by (3.17) is the possibility of separation effects in these flows.

3.1. *Recovery of the Ekman structure*

As just noted, once the slope f' drops below δ in magnitude, (3.16)–(3.18) above are not valid. In particular, note that rather different structures occur for the two cases noted above, namely large values of σS, or order-one values of that parameter. It is clear from (3.8) that the viscous terms do not enter, to leading order, if δ is bigger than ϵ (that is, $E^{\frac{1}{2}}$). So, in the 'non-diffusive' case ($\sigma S \gg 1$), where we noted the above scalings fail at $f' = O(\epsilon)$, the layer for f' in this range is an Ekman layer, though suitably modified for baroclinic vorticity production. We do not explore this case further, since it has little importance as noted above.

For the small-f' case noted explicitly above in (3.15) and (3.16) and for which σS is order one or smaller, it is evident from (3.8) that once $f' = O(\delta)$, the layer is not yet necessarily an Ekman layer if f' is still large compared with $E^{\frac{1}{2}}$. Indeed, in this case, writing $v = \delta\tilde{v}$, and $\rho = \epsilon\tilde{\rho}$ as required by (3.1), (3.8a) becomes

$$\frac{f'}{\delta}\frac{\partial \tilde{\rho}}{\partial y} - 2\frac{\partial \tilde{v}}{\partial y} = \frac{\partial \tilde{\rho}}{\partial r}, \tag{3.19}$$

which may not be integrated, as in (3.9) previously, to show that, on the surface, when $\tilde{\rho}$ vanishes, so does $\tilde{v}$. In fact, satisfying $\tilde{\rho} = 0$ at the surface means, in general, that $\tilde{v}$ is not zero there. Thus, there is a need for another (thinner) layer to satisfy no slip. That layer is a conventional Ekman layer, with width ϵ as usual. The density-layer equation, (3.5), is still appropriate at the outer layer. Choosing $\delta = (\lambda^2\epsilon/\sigma S)^{\frac{1}{3}}$, and also scaling w by δ^2, we obtain, from (3.5), the density-layer equation

$$\hat{u}\frac{\partial \tilde{\rho}}{\partial r} + \frac{\tilde{v}}{r}\frac{\partial \tilde{\rho}}{\partial \theta} + \tilde{w}\frac{\partial \tilde{\rho}}{\partial y} + \frac{1}{2}\frac{f'}{\delta}A^-\frac{\partial A^-}{\partial \theta} = \frac{\partial^2 \tilde{\rho}}{\partial y^2}, \tag{3.20}$$

and $\tilde{\rho}$ must approach $-A^-$ for $y \uparrow \infty$, with corresponding matching conditions on $\hat{u}$ and $\hat{v}$ derived from (3.1). This structure persists for values of f' smaller than δ, with the fourth term of (3.20), and the first of (3.19) absent. Notice that this boundary layer, in contrast to the one described by (3.17), is fully three-dimensional, incorporating convection in the radial direction – which is not present at larger f' values. Further, nothing special happens at f' values of order $E^{\frac{1}{2}}$ – the double-structured boundary layer persists to f' values of zero.

So, then, noting the layer width here, we see that for $\sigma S = O(1)$, the Ekman layer reappears, not at slopes of order $E^{\frac{1}{2}}$, but rather at slopes with the (larger) value of $E^{\frac{1}{6}}/(\sigma S)^{\frac{1}{3}}$.

4. The A-equations

The outer solutions presented in §2 satisfy density boundary conditions on the solid surfaces to *leading* order (cf. (2.7), (2.8), and (2.13)). However, the $\boldsymbol{u}_I$ velocities slip over the surface and $w_2 \neq 0$ at the surfaces. On the horizontal surfaces ($z = 1$, $z = 0$, $r > a$), conventional Ekman layers exist; ρ_1 is taken to zero at the boundaries *via* a layer of width $(E/\sigma Ro)^{\frac{1}{2}}$ which is thicker than the Ekman layer. The layers are essentially decoupled. Thus, on these surfaces the velocity components from the interior flow of §2 must satisfy the conventional Ekman compatibility conditions, hence

$$w = \mp \tfrac{1}{2} E^{\frac{1}{2}} \left[\frac{1}{r} \frac{\partial (rv)}{\partial r} - \frac{1}{r} \frac{\partial u}{\partial \theta} \right] \quad \text{on} \quad \begin{cases} z = 1, \\ z = 0, \quad r > a. \end{cases} \tag{4.1}$$

On the sloping surface $z = f(r)$, the situation is, as we have seen in §3, more of a problem. The component of outer flow velocity normal to the obstacle surface is

$$\frac{-f' u_1}{[1 + (f')^2]^{\frac{1}{2}}}. \tag{4.2}$$

If this fluid flows into the boundary layer, it leads to volumetric flow rates in the layer of order $f'/(\lambda \epsilon^{\frac{1}{2}})$ for $f' = O(1)$, and $O(\lambda^2 \epsilon |f'|^{\frac{1}{2}})^{-1}$ for $|f'|$ large. Since such a large flow rate seems impossible, we are led to the requirement that

$$u_1 = 0 \quad \text{on} \quad z = f(r). \tag{4.3}$$

If f' is small, on the other hand, the situation is quite different since, when $f' = O(E^{\frac{1}{6}})$, the boundary layer is once again an Ekman layer, so the flow rate in the layer is $O(1)$. In such an eventuality, (4.3) is replaced by a condition including Ekman suction. We leave such cases to subsequent work and proceed to the detailed analysis of the outer flow, first in $r > a$, then in $r < a$.

4.1. *Flow in $r > a$*

Combining the expansion (2.9) with the Ekman compatibility condition (4.1) and relating ϵ and E as given in (2.20) leads to the boundary conditions on w_2,

$$w_2 = \mp \lambda \tfrac{1}{4} \nabla_1^2 p_1 \quad \text{on} \quad z = \tfrac{1}{2} \pm \tfrac{1}{2}. \tag{4.4}$$

Recalling from §2 that there is no vortex stretching in the $(\,)_2$ flow so that $\partial w_2/\partial z = 0$, (4.4) indicates that

$$\nabla_1^2 p_1|_{z=0} + \nabla_1^2 p_1|_{z=1} = 0. \tag{4.5}$$

Substituting the solution (2.17) into this equation leads to

$$\nabla_1^2 (A^+ + 2B) = 0,$$

where A^+ shall hereafter denote A in the $r > a$ region. For convenience, let $B = -\frac{1}{2}A^+ + \phi$; then,

$$\nabla_1^2 \phi = 0, \quad r > a \tag{4.6}$$

so that (2.17) takes the special form

$$p_1 = (z - \tfrac{1}{2}) A^+ + \phi. \tag{4.7}$$

Equation (2.19) relates w_2 to A and B, so here it becomes

$$w_2 = \frac{1}{2r} \frac{\partial(A^+, \phi)}{\partial(r, \theta)}.$$

However, (4.4) also gives an expression for w_2 at $z = 1$ which, when combined with (4.7), leads to

$$w_2 = -\tfrac{1}{8}\lambda \nabla_1^2 A^+.$$

Equating these two expressions for w_2 results in the transport equation for A^+,

$$\frac{1}{r} \frac{\partial(\phi, A^+)}{\partial(r, \theta)} = \tfrac{1}{4}\lambda \nabla_1^2 A^+, \quad r > a. \tag{4.8}$$

So p_1 is obtained from (4.7), with A^+ and ϕ solutions of (4.8) and (4.6) respectively.

Far upstream, (2.5) indicates that

$$\left.\begin{aligned} A^+ &\to 0 \\ \phi &\sim -2r \sin\theta \end{aligned}\right\} \quad \text{for } r \to \infty. \tag{4.9}$$

4.2. *Flow in $r < a$*

Because of the large size of this obstacle, and the fact that the boundary condition (4.3) is a kinematic one, the form of solution (2.17) is considerably different from (4.7). In what follows, we first impose condition (4.2) to evaluate B in (2.17). Then, we construct an expression for the radial Ekman flux over the obstacle, and impose the condition that there be no *net* radial mass transport. That requirement further constrains the form of A^-. Finally, equating (2.19) to an expression for the fluid pumped out of the upper-surface Ekman layer results in an equation equivalent to (4.8), but for A^-.

Since $u_1 = -(1/2r)(\partial p_1/\partial\theta)$, (4.2) is

$$\frac{\partial}{\partial\theta}(B + fA^-) = 0,$$

the general solution of which is $B = -fA^-$ plus a function of r alone, which must be zero to match to the boundary-layer solution; see (3.9). Then, (2.17) becomes

$$p_1 = (z - f) A^-, \tag{4.10}$$

and w_2, from (2.19), is

$$w_2 = \frac{f' A^-}{2r} \frac{\partial A^-}{\partial\theta}. \tag{4.11}$$

Greenspan (1968, p. 46) gives an expression for the radial volumetric flow rate in the Ekman layer. Over the upper ($z = 1$) surface, it is

$$\mathscr{F}_t = -\tfrac{1}{2}\lambda\epsilon(u + v). \tag{4.12}$$

On the lower surface, we write again the flux law for the boundary layer discussed in §3, and given in particular by (3.12), (3.13), or (3.15), but in a more generic form:

$$\mathscr{F}_{\mathrm{b}} = \lambda^2 \epsilon q. \tag{4.13}$$

Since both u_1 and u_2 in the outer flow are proportional to θ-derivatives of p_1 and p_2, respectively, their integrals from zero to 2π in θ are zero, i.e. no net radial transport occurs in the geostrophic flow. Combining, then, (4.12) and (4.13), the total boundary-layer flow rate is

$$\mathscr{F}_{\mathrm{tot}} = \mathscr{F}_{\mathrm{t}} + \mathscr{F}_{\mathrm{b}} = \tfrac{1}{4}\lambda\epsilon\left(\frac{\partial p_1}{\partial r} - \frac{1}{r}\frac{\partial p_1}{\partial \theta}\right)\Big|_{z=1} + \lambda^2 \epsilon q. \tag{4.14}$$

Integrating in θ on $(0, 2\pi)$ causes the last term in (4.14) to vanish identically, and substitution of (4.10) leads to the no-net-radial-flow requirement,

$$\frac{\mathrm{d}}{\mathrm{d}r}[(1-f)\langle A\rangle] = 0, \tag{4.15}$$

where $\langle A\rangle$ denotes the θ-average of A^-. The solution of this equation is that $\langle A\rangle = \mathrm{const.}/(1-f)$. As we know from the discussion at the end of §3, provided the object is rounded at its centre – that is, $f'(0) = 0$, the boundary layer there will be, in fact, an Ekman layer; Greenspan (1968) notes that an axisymmetric swirling motion between parallel planes causes radial outflow in both Ekman layers, and hence is impossible since there is no source on the axis. Therefore, $\langle A\rangle$ must vanish for $r = 0$, and hence it vanishes for all r. So the solution of (4.15) is $\langle A\rangle \equiv 0$.

At $z = 1$, where there *is* an Ekman layer, (4.4) and (4.10) combine to give

$$w_2 = -\tfrac{1}{4}\lambda \nabla_1^2[(1-f)A^-]. \tag{4.16}$$

Combining with (4.11) gives the A^- equation

$$\frac{-f'A^-}{r}\frac{\partial A^-}{\partial \theta} = \tfrac{1}{2}\lambda \nabla_1^2[(1-f)A^-]. \tag{4.17}$$

Thus, to summarize, A^- is a solution of (4.17), recalling that the pressure, the stream function, is related through (4.10),

$$p_1 = (z-f)A^-. \tag{4.18}$$

We have found that the strong constraining influences of the Ekman suction on the horizontal boundaries and the kinematic boundary condition on the obstacle surface lead to particular forms for the pressure stream function in $r > a$ (equation (4.7)) and in $r < a$, over the top of the bump (equation (4.18)). Requiring that there be no vortex stretching to $O(\epsilon)$, the vertical velocity pumped out of the Ekman layers convects the mean density gradient to balance the convection of baroclinic density perturbations due to the thermal wind.

5. The viscous shear layer

The outer flow examined in §§2 and 4 is structurally quite different inside and outside the cylinder $r = a$ which circumscribes the obstacle. The two solutions (4.7) and (4.18) must be joined somehow at the common boundary, $r = a$. Choosing continuity and differentiability of p_1 on $r = a$ gives four conditions on three dependent variables, A^+, A^-, and ϕ, so the solution is overdetermined. To resolve the

matter, it is necessary to investigate the viscous shear layer that straddles $r = a$. Actually, two such layers are possible. A 'buoyancy layer' discussed by Barcilon & Pedlosky (1967) has width $E^{\frac{1}{2}}$ and is appropriate only for obstacles with vertical sides; here we have already supposed $|f'(a)| < \infty$, so this layer does *not* occur. A layer of width $E^{\frac{1}{3}}$ occurs here. We write

$$\rho = -z + \epsilon\bar{\rho} \tag{5.1}$$

in order to allow the layer to smooth the jump in ρ_1 that will always occur across $r = a$ (cf. (2.18)). Writing the other variables as

$$v = (E^{\frac{1}{2}}\lambda)^{-\frac{1}{3}}\bar{v}, \quad w = \frac{E^{\frac{1}{3}}}{\lambda^4}\bar{w}, \tag{5.2}$$

with $r - a = (E^{\frac{1}{2}}\lambda)^{\frac{1}{3}}\xi$, and substituting into (2.1)–(2.3) gives the shear-layer equations

$$\frac{\partial u}{\partial \xi} + \frac{1}{a}\frac{\partial \bar{v}}{\partial \theta} = 0, \tag{5.3}$$

$$\frac{\partial \bar{\rho}}{\partial \xi} + 2\frac{\partial \bar{v}}{\partial z} = 0, \tag{5.4}$$

$$\frac{\partial^3 \bar{v}}{\partial \xi^3} + 2\frac{\partial \bar{w}}{\partial z} = 0, \tag{5.5}$$

$$u\frac{\partial \bar{\rho}}{\partial \xi} + \frac{\bar{v}}{a}\frac{\partial \bar{\rho}}{\partial \theta} - \bar{w} = 0. \tag{5.6}$$

Matching these solutions to those of §§2 and 3 leads to boundary conditions on the solutions to (5.3)–(5.6),

$$\bar{v} \to 0, \quad \bar{w} \to 0, \quad |\xi| \to \infty, \tag{5.7a}$$

$$u \to u_1|_{r=a}, \quad |\xi| \to \infty, \tag{5.7b}$$

$$\bar{\rho} \to \rho_1|_{r=a}, \quad |\xi| \to \infty. \tag{5.7c}$$

Boundary conditions on $z = 0$ and $z = 1$ are determined by matching solutions of (5.3)–(5.6) to the Ekman layers on those boundaries. Substitution into (4.1) yields

$$\frac{\partial \bar{v}}{\partial \xi} = 0 \quad \text{on} \quad \begin{cases} z = 1, \\ z = 0, \ \xi > 0, \end{cases}$$

which may be integrated once, and in the light of (5.7a), becomes

$$\bar{v} = 0 \quad \text{on} \quad \begin{cases} z = 1, \\ z = 0, \ \xi > 0. \end{cases} \tag{5.8}$$

On the surface $z = f$, $z = f'(a)\,(E^{\frac{1}{2}}\lambda)^{\frac{1}{3}}\xi$ so, to *leading* order, the surface is on $z = 0$ if $f'(a)$ is finite. The kinematic condition (4.3) is still valid, so

$$u = 0 \quad \text{on} \quad z = 0, \ \xi < 0.$$

From this result, (5.3) shows that $\bar{v} = \bar{v}(\xi)$ on $z = 0$, $\xi < 0$. The volumetric flow rate in the Ekman layer on the surface in $\xi < 0$ is $O(E^{\frac{1}{3}})$ and is proportional to $\bar{v}|_{z=0,\,\xi<0}$, by (4.14). Since this flux must integrate over $(0, 2\pi)$ in θ to be zero, $\bar{v} \equiv 0$ is required and hence (5.8) is supplemented by

$$\bar{v} = 0 \quad \text{on} \quad z = 0, \ \xi < 0, \tag{5.9}$$

but leaves open the question of what happens precisely at $\xi = 0$. Notice that integration of (5.4) in ξ across the layer, and use of matching conditions (5.7) and boundary condition (5.8*a*) gives

$$\int_{-\infty}^{\infty} \bar{v}\,\mathrm{d}\xi = \tfrac{1}{2}(1-z)\,[\rho_1], \tag{5.10}$$

where the [ ] notation is defined by

$$[Z] = Z|_{r=a+} - Z|_{r=a-}.$$

Evaluating (5.10) at $z = 0$ and noting from (5.8*b*) and (5.9) that $\bar{v} = 0$ in $\xi < 0$ and $\xi > 0$ on $z = 0$, one concludes that $\bar{v}$ in fact must be singular at $\xi = 0$. Thus, we replace (5.8) and (5.9) with

$$\left.\begin{aligned} \bar{v} &= 0 \quad \text{on} \quad z = 1, \\ \bar{v} &= \tfrac{1}{2}[\rho_1]_{z=0}\,\delta(\xi) \quad \text{on} \quad z = 0 \end{aligned}\right\} \tag{5.11}$$

where $\delta(\xi)$ is the Dirac delta function in this instance. The solution to (5.3)–(5.6) under (5.7) and (5.11) is not easy, and we proceed to certain solution properties.

5.1. *Solution properties*

Appropriate solutions to the shear-layer equations do not exist unless ρ_1 and u_1 at $r = a\pm$ exhibit some particular properties. These constraints on ρ_1 and u_1 at $r = a$ result in the proper conditions for joining the solutions to (4.8) and (4.17), and hence amount to solvability conditions on the asymptotic structure. The particular technique used here of utilizing certain integrals of the equations of motion in the shear layer was first employed, to the knowledge of this author, by Stewartson (1966), and since used by other workers in rotating flows; particularly notable in this connection is the paper by Moore & Saffman (1969*b*). In the latter paper, no unique solution to the inviscid outer flow could be obtained without appeal to conservation of mass – much like the argument leading to Property 2 below. The best detailed discussion of the technique is found in Moore & Saffman (1969*a*).

1. *Continuity of u_1 at $z = 1$*

Integrate (5.3) in ξ across the layer. Making use of (5.7),

$$[u_1] + \frac{1}{a}\frac{\partial}{\partial\theta}\int_{-\infty}^{\infty} \bar{v}\,\mathrm{d}\xi = 0. \tag{5.12}$$

But (5.11) indicates $\bar{v} \equiv 0$ on $z = 1$. Thus, (5.12) gives the result that

$$[u_1] = 0 \quad \text{at} \quad z = 1. \tag{5.13}$$

2. *Constancy of vertical volume flow rate*

Integration of (5.5) across the layer (in ξ) gives, on requiring $\bar{v}$ and its derivatives to vanish, by (5.7) for $|\xi| \to \infty$,

$$\frac{\partial}{\partial z}\int_{-\infty}^{\infty} \bar{w}\,\mathrm{d}\xi = 0,$$

which indicates that, in particular,

$$\int_{-\infty}^{\infty} \bar{w}|_{z=0}\,\mathrm{d}\xi = \int_{-\infty}^{\infty} \bar{w}|_{z=1}\,\mathrm{d}\xi. \tag{5.14}$$

Since $w = O(E^{\frac{1}{3}})$ here and the layer has width $E^{\frac{1}{3}}$, the upward flow is $O(E^{\frac{1}{2}})$ (or $O(\epsilon)$), which is the order of the flow rates in the Ekman layers on the solid walls. In particular, the *net* radial influx of fluid into the shear layer at $z = 1$ is found by subtracting expressions (4.12) inside and outside of the layer. So, the net outflow is

$$-\tfrac{1}{2}\lambda\epsilon([u_1]+[v_1])|_{z=1}.$$

This fluid must enter the shear layer at $z = 1$, so it must be equal to

$$+\int_{-\infty}^{\infty} w\,\mathrm{d}(r-a) = +\epsilon\int_{-\infty}^{\infty} \bar{w}\,\mathrm{d}\xi.$$

Hence
$$\int_{-\infty}^{\infty} \bar{w}\,\mathrm{d}\xi = -\tfrac{1}{2}\lambda[v_1] \quad \text{at} \quad z = 1. \tag{5.15}$$

The *net* transport in the lower layers, using (4.12) and (4.13), is

$$-\tfrac{1}{2}\lambda\epsilon(u_1^+ + v_1^+)|_{z=0} + \lambda^2\epsilon q.$$

Again, this *must* be equal to

$$-\epsilon\int_{-\infty}^{\infty} \bar{w}\,\mathrm{d}\xi \quad \text{at} \quad z = 0,$$

so
$$\int_{-\infty}^{\infty} \bar{w}\,\mathrm{d}\xi = +\tfrac{1}{2}\lambda(u_1^+ + v_1^+ - \lambda q) \tag{5.16}$$

at $z = 0$. Then constancy of flow rate, (5.14), gives

$$[v_1]|_{z=1} + (u_1^+ + v_1^+ - \lambda q)|_{z=0} = 0. \tag{5.17}$$

3. *Global energy conservation*

Note that (5.6) may also be integrated across the layer. That results in

$$[\rho_1 u_1] + \frac{1}{a}\frac{\partial}{\partial\theta}\int_{-\infty}^{\infty} \overline{\rho v}\,\mathrm{d}\xi = \int_{-\infty}^{\infty} \bar{w}\,\mathrm{d}\xi.$$

If this is applied directly at $z = 1$ where $\bar{v} \equiv 0$ by (5.11), then it becomes

$$[\rho_1 u_1] = \int_{-\infty}^{\infty} \bar{w}\,\mathrm{d}\xi \quad \text{at} \quad z = 1.$$

However, $[u_1] \equiv 0$ at 1 by (5.13), and the integral is given by (5.15). Hence,

$$u_1[\rho_1] = -\tfrac{1}{2}\lambda[v_1] \quad \text{at} \quad z = 1. \tag{5.18}$$

Equations (5.13), (5.17), and (5.18) constitute solvability conditions for the shear layer. Since u_1, v_1, ρ_1 are related to p_1, and p_1 is given by (4.7) in $r > a$ and by (4.18) in $r < a$, each of these conditions may be written down in terms of A^+, ϕ, and A^-. That results in

1:
$$\tfrac{1}{2}A^+ - A^- + \phi = 0 \quad \text{on} \quad r = a, \tag{5.19}$$

2:
$$2\frac{\partial\phi}{\partial r} - \frac{\partial A^-}{\partial r} + \frac{1}{a}\frac{\partial[A]}{\partial\theta} + f'(a)A^- - \lambda q = 0 \quad \text{on} \quad r = a, \tag{5.20}$$

3:
$$\frac{[A]}{a}\frac{\partial A^-}{\partial\theta} + \tfrac{1}{2}\lambda\left[\frac{1}{2}\frac{\partial A^+}{\partial r} - \frac{\partial A^-}{\partial r} + \frac{\partial\phi}{\partial r} + f'(a)A^-\right] = 0. \tag{5.21}$$

The final term in (5.20) is a measure of how interactive the solution is, since q depends nonlinearly upon A^- through the relation with the Prandtl boundary layer on the sloping surface. We conclude that λq must be small in any solution without such interaction.

It is disconcerting that the shear-layer flow requires that u_1 be discontinuous at $r = a$. The reason is that the requirement that whatever mass erupts into the shear layer at its top ($z = 1$) must leave at its base ($z = 0$) forces the vertical velocity in the layer to be $O(\epsilon^{\frac{2}{3}})$, leading to $O(1)$ radial velocities. The u-discontinuity is, however, traceable to the large size of the obstacle. Were f' very small so that the surface boundary layer becomes an Ekman layer, an additional function, say ϕ^-, comes into the p_1 solution in $r < a$, so that continuity of the pressure and its radial derivative at $r = a$, leading to four joining conditions, is appropriate. In such a case, there is no Ekman-layer eruption into the shear layer, and the entire shear layer is much weaker – u_1 is obviously continuous in that case. (The author is grateful to a referee for helping to clarify this point.)

6. Stratification-dominated solution: $\lambda \to \infty$

The quantity λ, which in dimensional terms is given by $(\nu/\Omega^3)^{\frac{1}{2}} g\Delta\rho^*/U\rho_0^* h$, will be large for dominant stratification effects. We note, however, from (5.20) that a large λ the problem is highly nonlinear unless q is also small. Recall that for f' small, (3.14) indicates that $q = |f'(a)|Q$, so the analysis in this section is valid under stated restrictions in (3.16); hence we require that

$$\lambda^{\frac{2}{3}}(\epsilon/\sigma S)^{\frac{1}{3}} \ll |f'| \ll \frac{1}{\lambda}. \tag{6.1}$$

For $f' = O(1)$, it appears that the Prandtl boundary layer leads to strong nonlinearities, and in particular the strong possibility of separated flow. Apparently, if $\lambda \gg 1$, then *only* for obstacles with small slopes is it possible to proceed with a solution of the sort given below.

Letting $\lambda \to \infty$ under (6.1), then (4.8) and (4.17), together with the joining conditions (5.19), (5.20), and (5.21), to be applied at $r = a$ become

$$\nabla^2 A^+ = \nabla^2 \phi = 0 \quad \text{in} \quad r > a, \tag{6.2}$$

$$\nabla^2 (1-f) A^- = 0 \quad \text{in} \quad r < a, \tag{6.3}$$

$$\tfrac{1}{2} A^+ - A^- + \phi = 0 \quad \text{on} \quad r = a, \tag{6.4}$$

$$\left[\frac{\partial A}{\partial r}\right] - \frac{1}{a}\frac{\partial [A]}{\partial \theta} = -f'(a) A^- \quad \text{on} \quad r = a, \tag{6.5}$$

$$2\left(\frac{\partial \phi}{\partial r} - \frac{1}{a}\frac{\partial \phi}{\partial \theta}\right) = \left(\frac{\partial}{\partial r} - \frac{1}{a}\frac{\partial}{\partial \theta}\right)(1-f) A^- \quad \text{on} \quad r = a. \tag{6.6}$$

Solution, of the Stokes-like problem, is

$$\left.\begin{aligned} p_1^+ &= -2r\sin\theta + 2\frac{a^2(1-z)}{r}\cos\theta \\ p_1^- &= -\frac{z-f}{1-f} 2r\sin\theta. \end{aligned}\right\} \tag{6.7}$$

We show, in figure 2, streamlines for solution (6.7).

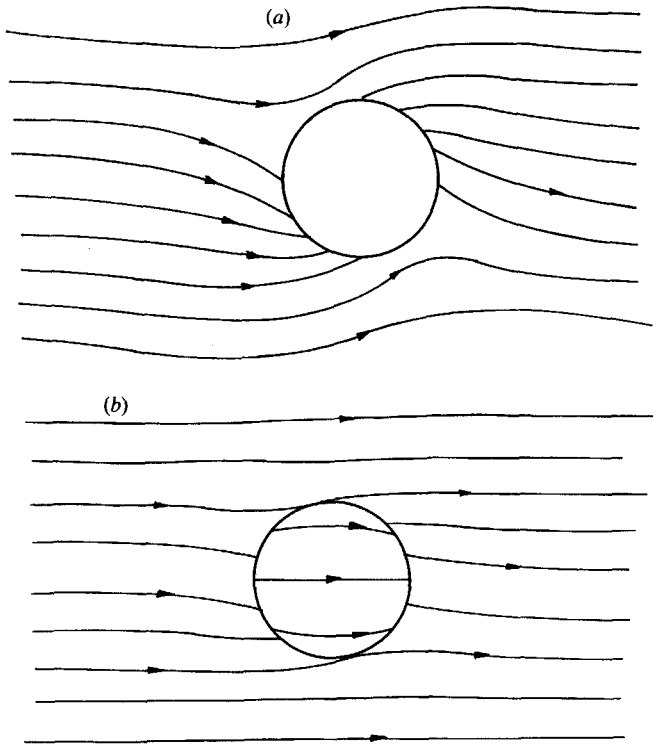

FIGURE 2. Stratification-dominated flow past a paraboloid with maximum height $\frac{1}{4}$. (*a*) Streamlines in the $z = 0$ plane. (*b*) Streamlines in the $z = \frac{3}{4}$ plane. p_1 interval between streamlines is 0.25.

The solution (6.7) actually represents the leading terms in a series of inverse powers of λ:

$$\left.\begin{aligned} A^+ &= A_1^+ + (1/\lambda)A_2^+ + \ldots, \\ A^- &= A_1^- + (1/\lambda)A_2^- + \ldots, \\ \phi &= \phi_1 + (1/\lambda)\phi_2 + \ldots. \end{aligned}\right\} \tag{6.8}$$

Substitution of (6.8) into (4.8), (4.17), (5.19), (5.20), and (5.21) leads to the equations and boundary conditions for the second-order solution, denoted by subscript 2; we omit those equations for the sake of brevity and simply give the solutions, whose construction is a straightforward exercise:

$$A_2^+ = 4a^2\left[\left(\frac{a}{r}\right)^2 - 1\right]\cos(2\theta) - 2\left(\frac{a^4}{r^2}\right)\left(1 + \frac{P'(a)}{4a}\right)\sin(2\theta) - 8a^2\log\left(\frac{r}{a}\right) - 2\phi_2, \tag{6.9}$$

$$(1-f)A_2^- = \left[P(r) - \frac{1}{4}\left(\frac{r^2}{a}\right)P'(a) - r^2\right]\sin(2\theta), \tag{6.10}$$

$$\phi_2 = \tfrac{1}{20}[(aP'(a) - 12a^2)\cos(2\theta) - (3aP'(a) + 4a^2)\sin(2\theta)]\left(\frac{a}{r}\right)^2 \tag{6.11}$$

In this set of solutions, $P(r)$ is the particular solution of

$$\frac{1}{r}\frac{\mathrm{d}}{\mathrm{d}r}r\frac{\mathrm{d}P}{\mathrm{d}r} - \frac{4P}{r^2} = -\frac{4rf'(r)}{(1-f)^2}$$

that satisfies the condition $P(a) = 0$.

The expansion in (6.8) for A^+ is not uniformly valid for $r \to \infty$, as one may note from the fact that A_2^+, in (6.9), is $O(\log r)$ for $r \to \infty$, whereas A_1^+, from (6.6), is $O(1/r)$. In fact, for $r \to \infty$, (4.8) becomes the Oseen equation

$$\nabla^2 A^+ = \frac{8}{\lambda}\frac{\partial A^+}{\partial x}. \tag{6.12}$$

If $X = x/\lambda$ and $R = r/\lambda$, then the solution of (6.12) that is regular in $r > a$ is

$$\hat{A}^+ = \exp(4X) \sum_{n=0}^{\infty} (a_n \cos(n\theta) + b_n \sin(n\theta)) K_n(4R), \tag{6.13}$$

where K_n is a modified Bessel function of the second kind. By matching this solution for $R \to 0$ with the expansion (6.8) for $r \to \infty$, the Fourier coefficients in (6.13) may be determined. The result is that the solution of (4.9), valid for $R = O(1)$, is

$$\hat{A}^+ = -8(a^2/\lambda)(K_0(4R) + \tfrac{1}{2}\cos\theta K_1(4R)) \exp(4X). \tag{6.14}$$

It is instructive to examine the form of (6.14) for $R \to \infty$. Using the asymptotic forms for the modified Bessel functions,

$$A^+ = -4\frac{a^2}{\lambda}(1 + \tfrac{1}{2}\cos\theta)\left[\frac{\frac{1}{2}\pi}{R}\right]^{\frac{1}{2}} \exp(4(X-R)) \quad \text{for } \frac{r}{\lambda} \to \infty, \tag{6.15}$$

from which it is obvious that the solution contains a narrow wake far downstream of the obstacle, aligned with the upstream flow direction. A little examination of (6.15) shows the wake to have thickness proportional to $(\lambda x)^{\frac{1}{2}}$, which is small compared with the distance from the object provided that the conditions of (6.15) are satisfied, viz. $x \gg \lambda$. (Notice, however, that there is no wake structure in ϕ, so that on the centreline of the layer, $z = \frac{1}{2}$, there is no wake; forward flow in $z > \frac{1}{2}$ means rearward flow in $z < \frac{1}{2}$.)

7. The rotation-dominated solution: $\lambda \to 0$

If the λ-parameter is small, rotation effects dominate stratification effects. The limits of (4.8) and (4.17) for $\lambda \to 0$ are singular. The outer solutions are particularly trivial; it is evident that

$$A^+ = o(1), \quad A^- = o(1) \quad \text{for } \lambda \to 0,$$

but ϕ must be $O(1)$ from boundary condition (4.9). That being the case, ϕ is an harmonic function satisfying $\phi = 0$ on $r = a$, from the limit of (5.19) for $\lambda \to 0$. Thus,

$$\phi = -2\sin\theta\left(r - \frac{a^2}{r}\right). \tag{7.1}$$

So, in the midplane, $z = \frac{1}{2}$, (4.7) and (7.1) indicate that the flow is the usual flow past a circular cylinder.

Since the $\lambda \to 0$ limit is singular, thin shear layers exist on both sides of $r = a$, sandwiching the layer of §4 between them. For $f'(a) = O(1)$, (5.20) indicates that $\partial A^-/\partial r$ should be $O(1)$. Also, (5.21) gives $[A] = 0$ at $r = a$ inside the layers, so A^+ and A^- are of the same order of magnitude. Thus, write $A^- = (-32a\lambda/f'(a))^{\frac{1}{3}} B^-$ and $r - a = (-\lambda a/16f'(a))^{\frac{1}{3}}\eta_-$. Equations (4.17) and (5.20) become

$$B^- \frac{\partial B^-}{\partial \theta} = \frac{\partial^2 B^-}{\partial \eta_-^2} \quad \text{in} \quad \eta_- < 0, \tag{7.2}$$

$$\frac{\partial B^-}{\partial \eta_-} = -\sin\theta \quad \text{on} \quad \eta_- = 0. \tag{7.3}$$

It is easily shown that the solution to this problem develops from $\theta = \pi$ to $\theta = 0$ or $\theta = 2\pi$ on either side of the cylinder.

Once B^- is obtained, A^+ may be found from $A^+ = (-32\lambda a/f'(a))^{\frac{1}{3}} B^+$, where B^+ is a solution of a heat equation,

$$\frac{\partial B^+}{\partial s} = \frac{\partial^2 B^+}{\partial \xi^2} \quad \text{in} \quad s > 0, \tag{7.4}$$

which is obtained from (4.8) under the scaling $r - a = \frac{1}{2}(\lambda a)^{\frac{1}{3}}\eta_+$, and with the transformations $\xi \equiv \eta_+ \sin\theta$, $s \equiv 1 + \cos\theta$. As noted above, the boundary condition from (5.21) is

$$B^+ = B^- \quad \text{on} \quad \xi = 0 \tag{7.5}$$

and, since the layers develop from $\theta = \pi$,

$$B^+ = 0 \quad \text{on} \quad s = 0, \quad \text{all } \xi. \tag{7.6}$$

A series solution for B^- may be constructed, the first two terms of which are

$$B^- = \frac{\theta - \pi}{Y^2} + \frac{(\pi - \theta)^3}{6q}\frac{Y_0^{q+1}}{Y^q} + O(\pi - \theta)^5, \tag{7.7}$$

where $Y(\eta) \equiv (\frac{2}{3})^{\frac{1}{6}} - \eta_-/\sqrt{6}$, $Y_0 \equiv Y(0)$, and $q = \frac{1}{2}(\sqrt{97} - 1)$. In similar fashion, using (7.5), (7.4) may be solved by a series, which begins

$$B^+ = -(\tfrac{3}{2})^{\frac{1}{3}}(2\pi s)^{\frac{1}{2}}\,\mathrm{i}^1\mathrm{erfc}\,(\xi/2s^{\frac{1}{2}}) + \tfrac{1}{2}\pi^{\frac{1}{2}}\frac{(q-2)}{14^{\frac{2}{3}}}(2s)^{\frac{3}{2}}\mathrm{i}^3\mathrm{erfc}\,(\xi/2s^{\frac{1}{2}}) + O(s^{\frac{5}{2}}), \tag{7.8}$$

where the members of the error function family may be found in Abramowitz & Stegun (1965).

Numerical solutions may also be obtained by standard Crank–Nicholson techniques. We show η-derivatives of B^+ and B^- evaluated at $\eta_\pm = 0$ in figure 3; boundary-layer thickness functions and are shown in figure 4. These thicknesses,

$$\int_{-\infty}^{0} \{B^-(\eta,\theta)/B^-(0,\theta)\}\,\mathrm{d}\eta, \quad \int_0^{\infty} \{B^+(\eta,\theta)/B^+(0,\theta)\}\,\mathrm{d}\eta,$$

from (7.7) and (7.8), begin at $\sqrt{6}$ and $\frac{1}{2}(\pi s)^{\frac{1}{2}}$ near $\theta = \pi$. Recall that B^+ and B^- represent density perturbations; their η-derivatives are vertical shears of azimuthal speeds in the layers.

8. Rotation-dominated solution past an obstacle with steep sides

The solution given in §7 is not uniformly valid for $|f'(a)| \to \infty$. In many laboratory situations, $f'(a)$ may be quite large. In addition, the author has not been able to construct a non-separated flow solution of the kind presented here in the case that the obstacle has vertical sides. It seems likely that as $|f'(a)|$ gets progressively larger, the structure of the A^+ and A^- boundary layers alters, and the solution fails to exist, indicating that flow separation may, in fact, have occurred. It is, then, with a view toward this separation that we construct, in this section, solutions of the A-equations for $\lambda \to 0$ and $f'(a) \to \infty$.

The slope of the obstacle comes into the problem through the boundary conditions,

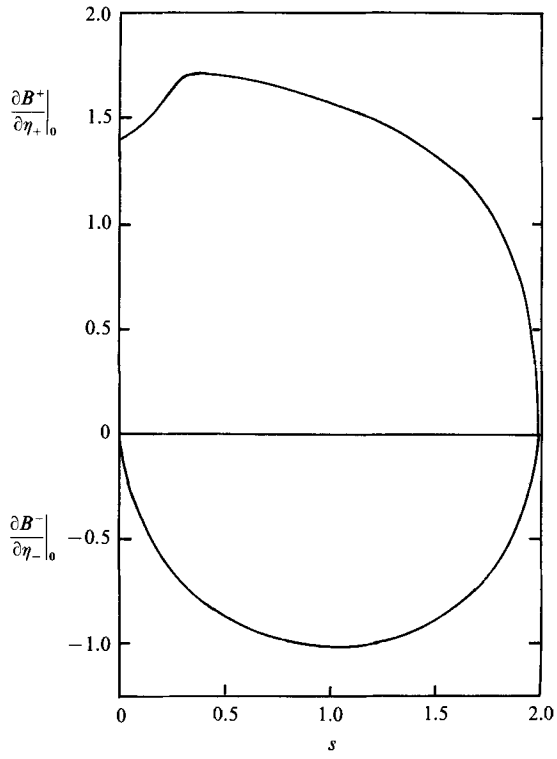

FIGURE 3. Taylor-column surface speed on $\eta_+ = 0$ and on $\eta_- = 0$ *vs.* distance, s, around the column. $\lambda a \ll 1$ and $\mu = O(1)$.

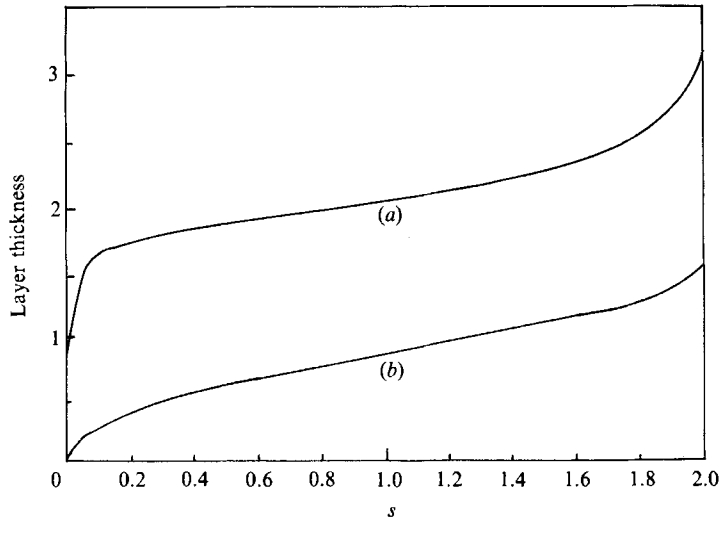

FIGURE 4. An integral measure of the rotational layer widths. (*a*) Inside the column, (*b*) outside the column. $\lambda a \ll 1$ and $\mu = O(1)$.

(5.19)–(5.21), but also directly into the equation (4.17). It is this latter occurrence that really complicates the analysis. In fact, the details of the obstacle shape near $r = a$ are crucial in determining the form of the A^- boundary layer there. For definiteness, consider an obstacle which is a spherical cap. The $f(r)$ appropriate to such a shape is given by

$$f(r) = -a + [a^2(\mu^2+1) - r^2]^{\frac{1}{2}}, \tag{8.1}$$

where we have now written μ for the value $-1/f'(a)$. If we evaluate $f'(r)$, which occurs in (4.17), in a thin layer near $r = a$ by writing, as in §7, $r - a = \delta\eta_-$, then it becomes, for $\delta \to 0$,

$$f'(r) \sim \frac{-a}{[\mu^2 a^2 - 2a\eta_- \delta]^{\frac{1}{2}}}. \tag{8.2}$$

Now, depending on the relative size of μ^2 and the layer thickness δ, f' takes on quite a different form so far as the boundary-layer approximation to (4.17) is concerned. Noting the boundary condition (5.20), and assuming that A^+ and A^- are $o(1)$ in the small parameters, we write $A^- = 8\delta B^-$. The boundary condition (5.20) then becomes, as $\lambda \to 0$ and $\mu \to 0$,

$$\frac{\partial B^-}{\partial \eta_-} = -\sin\theta \quad \text{on} \quad \eta_- = 0. \tag{8.3}$$

The other A^- term in (5.20) is negligible only if $\delta \ll \mu^{\frac{3}{2}}$. Note that (7.1) has been employed again as well. Equation (4.17), under these limits, then becomes

$$B^- \frac{\partial B^-}{\partial \theta} = \frac{\partial^2 B^-}{\partial \eta_-^2}, \tag{8.4}$$

where the layer thickness turns out to be $\delta = (\lambda a \mu/16)^{\frac{1}{3}}$. The condition mentioned above, below (8.3), requires that λa be small compared to $\mu^{\frac{7}{2}}$; however, the requirement from (8.2) means that λa must be much less than μ^5, which is the more restrictive requirement. Therefore, (8.4) may be solved under (8.3) only if

$$\lambda a \ll \mu^5. \tag{8.5}$$

The A^+ equation and boundary condition for this parameter range may be deduced as follows. The limit form of (5.21) under the scalings for A^- given above is simply

$$B^+ = B^- \quad \text{on} \quad \eta_+ = 0 \tag{8.6}$$

if $A^+ = 8\delta B^+$. Restriction (8.5) applies to this as well. B^+ obeys (7.4) with $\eta_+ = (r-a)/(\lambda a/16)^{\frac{1}{2}}$ as there. Hence, though the scalings for A^- differ a bit, the solution described in §7 still applies to this case.

8.1. $\mu^5 \ll \lambda a \ll \mu^{\frac{5}{2}}$

For values of λa larger than μ^5, the approximation for $f'(r)$ in (4.17) as $-1/\mu$ is no longer valid. In fact, in this case the $2a\delta\eta_-$ term in (8.2) now dominates. That being the case, we still write $A^- = 8\delta B^-$, but now δ is given by $\delta = (\lambda^2 a/128)^{\frac{1}{5}}$. The limit of (4.17), noting (7.2), is then

$$\frac{1}{(-\eta_-)^{\frac{1}{2}}} B^- \frac{\partial B^-}{\partial \theta} = \frac{\partial^2 B^-}{\partial \eta_-^2}. \tag{8.7}$$

Provided that λa is small compared with $\mu^{\frac{5}{2}}$, boundary condition (5.20) remains (8.3) in the limit. The B^+ equation and boundary condition continue to be given by (7.4) and (8.6) respectively. However, the B^+ solution is now certainly different since the value of B^- on $\eta_- = 0$ is now changed.

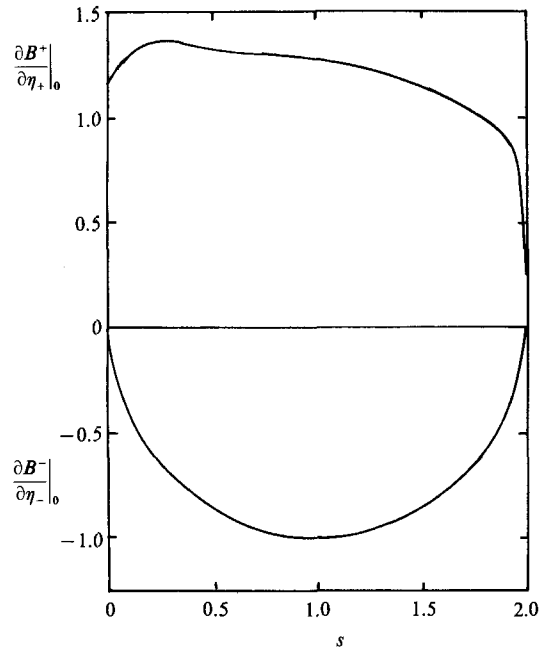

FIGURE 5. Taylor-column surface speed on $\eta_+ = 0$ and on $\eta_- = 0$ *vs.* distance, s, around the column. $\mu^5 \ll \lambda a \ll \mu^{\frac{5}{2}}$.

The solution to (8.7) under (8.3) may be expanded in a series away from $\theta = \pi$ as in §6. That series begins as

$$B^- = -(\pi-\theta)F_0(-\eta_-)+\tfrac{1}{6}(\pi-\theta)^3 F_1(-\eta_-)+\ldots. \tag{8.8}$$

The boundary condition requires that $F_0'(0) = F_1'(0) = 1$. The equation for $F_0(z)$ is given by

$$z^{\frac{1}{2}}F_0'' = F_0^2, \tag{8.9a}$$

and the F_1 equation is

$$z^{\frac{1}{2}}F_1'' = \tfrac{7}{6}F_0F_1. \tag{8.9b}$$

Solutions are difficult, but it is easily shown that, for $z \to 0$,

$$F_0 = c_1 - z + \tfrac{4}{3}z^{\frac{3}{2}}c_1^2 + \ldots,$$

$$F_1 = c_2 - z + \tfrac{7}{9}z^{\frac{3}{2}}c_1c_2 + \ldots,$$

and, for $z \to \infty$, at the edge of the layer,

$$F_0 \sim \tfrac{15}{4}z^{-\frac{3}{2}}; \quad F_1 \sim c_3 z^{-b}, \quad b = \tfrac{1}{2}(\sqrt{111}/6 \sim 1).$$

The constants c_1, c_2, and c_3 are not arbitrary. In fact, integrating (8.9) across the boundary layer gives the integral conditions

$$\int_0^\infty F_0^2/z^{\frac{1}{2}}\,\mathrm{d}z = 1, \quad \int_0^\infty F_0F_1/z^{\frac{1}{2}}\,\mathrm{d}z = \tfrac{6}{7}.$$

(c_1, c_2, c_3) are related to these constraints. Obviously the B^+ solution proceeds in much the same fashion here as in §7. The result is a solution that is very like (7.8), with constants c_1 and c_2 appearing as multipliers on the terms. Numerical solutions for (7.4) and (8.7) are shown in figures 5 and 6, namely, η-derivatives of B^+ and B^- on $\eta = 0$, and 'thicknesses', as discussed at the end of §7.

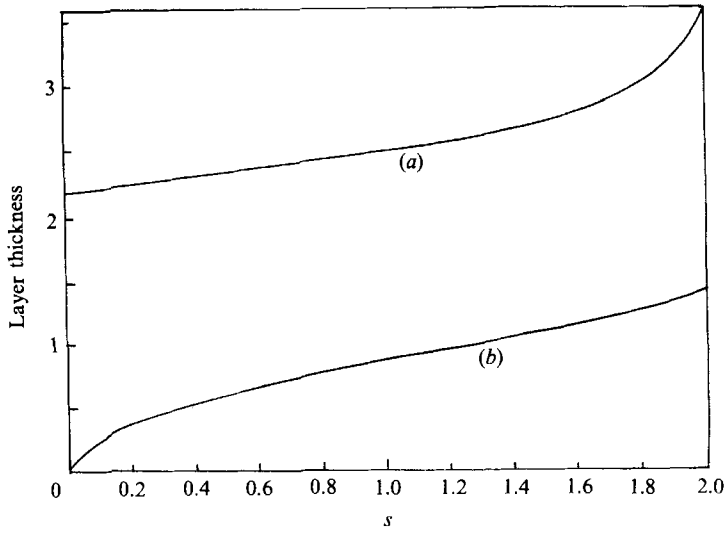

FIGURE 6. An integral measure of the rotational layer widths. (*a*) Inside the column, (*b*) outside the column. $\mu^5 \ll \lambda a \ll \mu^{\frac{5}{2}}$.

For λa of order $\mu^{\frac{5}{2}}$ and larger, the boundary condition (5.20) has a limit different from (8.3), viz.

$$B^- = -\sin\theta \quad \text{on} \quad \eta_- = 0. \tag{8.10}$$

Up to values of λa of the order of μ^2, however, the boundary condition (5.21) is modified, and the analysis is quite different. We proceed to that case.

8.2. $\mu^{\frac{5}{2}} \ll \lambda a \ll \mu^2$.

In this range, we write

$$A^+ = 8\mu B^+, \quad A^- = 8\mu B^-, \tag{8.11}$$

and the interior boundary layer, owing to the change in scale of A^-, now has a thickness given by $\delta = (\lambda^2 a/(128\mu^2))^{\frac{1}{3}}$. The equations for B^+ and B^- remain (7.4) and (8.7) respectively, and B^- satisfies (8.10) on $\eta_- = 0$. However, (5.21) in this limit becomes

$$p\frac{\partial B^+}{\partial \xi} + \frac{1-s}{(2s-s^2)^{\frac{1}{2}}}B^+ = 1-s+2p^2 \quad \text{on} \quad \xi = 0, \tag{8.12}$$

where $p = (\lambda a)^{\frac{1}{2}}/(16\mu)$, which is small in the parameter range.

Since p is $o(1)$, the limit of (8.12) is simply

$$B^+ = [2s-s^2]^{\frac{1}{2}} \quad \text{on} \quad \xi = 0. \tag{8.13}$$

The solution may proceed in series expansion for B^+ in powers of $s^{\frac{1}{2}}$ or it *may* be done numerically. The B^+ problem, (7.4) and (8.13), is clearly well-posed and there is no difficulty in completing the solution. However, close inspection of (8.12) shows that things are not so straightforward as they seem. Equation (8.13) is *not* the uniformly valid limit of (8.12) for $p \to 0$. There is a non-uniformity in the neighbourhood of $s = 1$ where the first derivative term in the boundary condition must be retained. In that small region near $s = 1$, write

$$B^+ = 1 + b(x, y), \quad \xi = (\sqrt{2}p)^{\frac{1}{3}}y, \quad s = 1 + (\sqrt{2}p)^{\frac{2}{3}}x. \tag{8.14}$$

The limit of (7.4) and (8.12) as $p \to 0$ then gives

$$\frac{\partial b}{\partial x} = \frac{\partial^2 b}{\partial y^2} \quad \text{for} \quad -\infty < x < \infty, \tag{8.15}$$

$$\frac{\partial b}{\partial y} = xb \quad \text{on} \quad y = 0. \tag{8.16}$$

Matching carefully to the solution to (7.4), (8.13) that is valid to left, right, and above this region, we conclude that $b \to 0$ for $x^2 + y^2 \to \infty$.

Now, clearly this problem is not well-posed. Here, we demonstrate the consequent non-uniqueness of the solutions of (8.15), (8.16), by construction of an eigenfunction. Generalizing the Laplace transformation, if the integration path is the imaginary axis in the t-plane, one solution to (8.15), (8.16) is

$$b = \frac{1}{2\mathrm{i}} \int_\Gamma \exp\left(tx + \tfrac{2}{3}t^3 - t^{\frac{1}{2}} y\right) \mathrm{d}t. \tag{8.17}$$

Any multiple of this solution is *also* a solution. Γ may be deformed for convenience so long as $\pi > |\arg t| \geqslant \frac{1}{3}\pi$, since a branch line lies on the negative real axis. Deforming the contour round the branch cut,

$$b = \int_0^\infty \mathrm{e}^{-rx} \sin\left(\tfrac{2}{3}r^{\frac{3}{2}} + r^{\frac{1}{2}} y\right) \mathrm{d}r \quad \text{in} \quad x > 0 \tag{8.18}$$

and using $\arg t = \pm \frac{1}{3}\pi$ for $x < 0$, we may also find

$$b = \int_0^\infty \exp\left(\tfrac{1}{2}rx - \tfrac{3}{2}r^{\frac{1}{3}} y\right) \sin\left(\tfrac{2}{3}r^{\frac{3}{2}} - \tfrac{1}{2}r^{\frac{1}{2}} y + \tfrac{\sqrt{3}}{2}rx + \tfrac{1}{3}\pi\right) \mathrm{d}r \quad \text{in} \quad x < 0. \tag{8.19}$$

Steepest-descent techniques may be applied to the integral (8.17); there are two critical points, but with the t-plane cut as indicated above, only one lies in $(-\pi, \pi)$ – one on the positive real axis. Deforming the Γ-contour to pass through that point gives the asymptotic form of b for $|x|$ and/or y large, viz.

$$b \sim \left[\frac{\pi}{2\tau}(\tau - \tfrac{1}{2}x)\right]^{\frac{1}{2}} \exp\left[-\tfrac{4}{3}(\tau - \tfrac{1}{2}x)^2 (\tau + \tfrac{1}{4}x)\right], \tag{8.20}$$

where $\tau \equiv (\frac{1}{2}y + \frac{1}{4}x^2)^{\frac{1}{2}}$. Specializing,

$$b \sim (-x\pi)^{\frac{1}{2}} \exp\left(\tfrac{1}{4}x^3\right), \quad x \to -\infty,$$

$$b \sim \left(\frac{\pi}{8x^3}\right)^{\frac{1}{2}} y \exp\left[-\tfrac{3}{16}(y^2/x)\right], \quad x \to +\infty,$$

and

$$b \sim \tfrac{1}{2}\pi(\tfrac{1}{2}y)^{\frac{1}{4}} \exp\left[-(\tfrac{1}{2}y)^{\frac{3}{2}}\right], \quad y \to \infty, \quad x = O(1).$$

So, in this parameter range, there is a tiny region near $s = 1$ in which the B^+ problem is ill-posed. As p grows, the trouble moves upstream from $s = 1$ toward $s = 0$.

The difficulty in this parameter range is worse than that, however, since inspection of (8.10) together with (3.17) shows that the boundary layer under the inner (B^-) shear layer is mathematically identical to the classical boundary layer on a circular cylinder in a potential flow, i.e. the fluid will separate from the surface in this narrow region under the shear layer – even though the B^- solution, itself, is well-behaved. It

is, in fact, the change in the B^- boundary condition from (8.3) to (8.10), for slopes larger than $(\lambda a)^{-\frac{2}{5}}$, that leads to the separation under the shear layer. Hence, in the parameter range at hand, separation occurs in a thin region round the rim of the bump, as a small zone of non-uniqueness develops just outside the column. One would anticipate, then, in this regime, that the entire solution structure is incorrect. Clearly the B^- solution and its boundary layer must be found interactively, with apparently some effect on the B^+ layer in the shoulder region. It seems that no massive separation, round all of the column, occurs at these slopes – perhaps it does at larger slopes.

To summarize the analysis of this section, we have found that for steep-sided obstacles, all of the vertical shear is confined in thin layers sandwiching the $E^{\frac{1}{6}}$ layer on $r = a$. As the slope, $f'(a)$, continues to increase, the structure of the layers alters through several regimes, until $f'(a)$ is of order $(\lambda a)^{-\frac{2}{5}}$, beyond which trouble first develops in the outer layer, in the form of non-uniqueness in the solution near the obstacle shoulders and the separation of the boundary layer under the interior shear layer.

Further investigation of the detailed nature of the separated flow, as well as numerical solutions for $\lambda = O(1)$, await a subsequent paper.

This material is based upon work supported by the National Science Foundation under grant number ATM-8417646. The author is particularly grateful to three referees for their comments on earlier versions of this paper.

REFERENCES

Abramowitz, M. & Stegun, I. 1965 *Handbook of Mathematical Functions*. Dover.

Baines, P. G. & Davies, P. A. 1980 Laboratory studies of topographic effects in rotating and/or stratified flows. In *Orographic Effects in Planetary Flows*, GARP Series 23, World Meteorological Organization, Geneva.

Barcilon, V. & Pedlosky, J. 1967 A unified theory of homogeneous and stratified rotating fluids. *J. Fluid Mech.* **29**, 609.

Boyer, D. L. & Biolley, F. M. 1986 Linearly-stratified, rotating flow over long ridges in a channel. *Phil. Trans. R. Soc. Lond.* A **318**, 411.

Boyer, D. L. & Chen, R. 1987 On the laboratory simulation of mountain effects on large-scale atmospheric motion systems: the Rocky Mountains. *J. Atmos. Sci.* **44**, 100.

Boyer, D. L., Davies, P. A. & Holland, W. R. 1984 Rotating flow past disks and cylindrical depressions. *J. Fluid Mech.* **141**, 67.

Boyer, D. L., Davies, P. A., Holland, W. R., Biolley, F. & Honji, H. 1987 Stratified rotating flow over and around isolated three-dimensional topography. *Phil. Trans. R. Soc. Lond.* A **322**, 213.

Cheng, H. K., Hefazi, H. & Brown, S. N. 1984 The cyclonic disturbance and lee waves above an obstacle in a stratified rotating fluid. *J. Fluid Mech.* **141**, 431.

Crissali, A. J. & Walker, J. D. A. 1976 Non-linear effects for the Taylor-column problem for a hemisphere. *Phys. Fluids* **19**, 1661.

Davies, P. A. 1972 Experiments on Taylor columns in rotating stratified fluids. *J. Fluid Mech.* **54**, 691.

Foster, M. R. 1979*a* Coriolis-force attenuation of blocking in a stratified flow. *J. Fluid Mech.* **94**, 711.

Foster, M. R. 1979*b* Vertical Stewartson layers in a stratified flow. *J. Mech. Appl. Maths* **32**, 339.

Foster, M. R. 1982 Slow rotating stratified flow past obstacles of large height. *Q. J. Mech. Appl. Maths* **35**, 509.

Greenspan, H. P. 1968 *The Theory of Rotating Fluids*. Cambridge University Press.

Hogg, N. 1973 On the stratified Taylor column. *J. Fluid Mech.* **58**, 517.

HUPPERT, H. E. 1975 Some remarks on the initiation of inertial Taylor columns. *J. Fluid Mech.* **67**, 397.

MCCARTNEY, M. S. 1975 Inertial Taylor columns on a beta plane. *J. Fluid Mech.* **68**, 71.

MERKINE, L. O. 1985 A linear analysis of rotating stratified flow past a circular cylinder on an *f*-plane. *J. Fluid Mech.* **157**, 501.

MOORE, D. W. & SAFFMAN, P. G. 1969*a* The structure of free vertical shear layers in a rotating fluid and the motion produced by a slowly rising body. *Phil. Trans. R. Soc. Lond.* A **264**, 597.

MOORE, D. W. & SAFFMAN, P. G. 1969*b* The flow induced by the transverse motion of a thin disk in its own plane through a contained rapidly rotating viscous liquid. *J. Fluid Mech.* **39**, 831.

SMITH, F. T. 1985 A structure for laminar flow past a bluff body at high Reynolds number. *J. Fluid Mech.* **155**, 175.

STEWARTSON, K. 1966 On almost rigid rotations. Part 2. *J. Fluid Mech.* **26**, 131.

WALKER, J. D. A. & STEWARTSON, K. 1974 The Taylor column problem for a hemisphere. *J. Fluid Mech.* **66**, 767.